Computers and Mathematics with Applications 61 (2011) 3246–3257

Contents lists available at ScienceDirect

Computers and Mathematics with Applications

journal homepage: www.elsevier.com/locate/camwa

Spatial attrition modeling: Stability conditions for a $2D + t$ FD formulation

Eduardo González *, Marcelo J. Villena

Faculty of Engineering and Sciences, Universidad Adolfo Ibáñez, Santiago, Chile

ARTICLE INFO

Article history:
Received 28 June 2010
Received in revised form 16 February 2011
Accepted 5 April 2011

Keywords:
PDE
Stability
Reaction–diffusion
Spatial attrition modeling

ABSTRACT

A new general formulation for the spatial modeling of combat is presented, where the main drivers are movement attitudes and struggle evolution. This model in its simplest form is represented by a linear set of two coupled partial differential equations for two independent functions of the space and time variables. Even though the problem has a linear shape, non-negative values for the two functions render this problem as nonlinear. In contrast with other attempts, this model ensures stability and theoretical consistency with the original Lanchester Equations, allowing for a better understanding and interpretation of the spatial modeling. As a numerical illustration a simple combat situation is developed. The model is calibrated to simulate different troop movement tactics that allow an invader force to provoke maximum damage at a minimum cost. The analysis provided here reviews the trade-off between spatial grid and time stepping for attrition cases and then extends it to a new method for guaranteeing good numerical behavior when the solution is expected to grow along the time variable. There is a wide variety of spatial problems that could benefit from this analysis.

1. Introduction

Lanchester [1] introduced a set of linear and only time-dependent differential equations that describes an attrition conflict between two opposite forces concentrated on a spot [2]. Since then, Lanchester Equations (LEs) have been widely used to model and theorize about combat attrition for many years. See for example [3,4], for earlier analysis and [5–7] for some recent contributions. A complete review can be found at [8]. This success can be explained mainly because of the simplicity of LEs, and the fact that they are very intuitive and hence easy to apply. Additionally, at present there are several research lines using LEs to analyze very different problems: such as behavioral ecology [9], epidemiology [10], infectology [11,12], marketing [13–17] and economics [18–21], which have maintained the interest in the Lanchester approach.

However, the traditional Lanchester approach lacks a spatial description. Some models have been developed, for example [22] makes an analogy with Reaction–Diffusion equation but constrained to one spatial dimension while leaving the identification of the parameters as an open-ended problem. The numerical solution to the extended mathematical formulation is then analyzed by [23], focusing mainly on the abstract problem. Later on, in another work, [24] analyze a specific nonlinear situation closely related to the Lanchester spatial formulation, but applied to predator–prey dynamics. Finally, another example deals with competition–diffusion, through the Lotka–Volterra formulation making emphasis on the spatial evolution of the competing species (see [25]). Adding to that research, a new formulation is introduced here, where the balance of forces yields a set of two coupled $2D + t$ PDEs. Particularly, this new formulation ensures stability and

* Corresponding author. Tel.: +56 23311269.
E-mail addresses: eduardo.gonzalez@uai.cl, e.gonzalez@ieee.org (E. González).

0898-1221/$ – see front matter
doi:10.1016/j.camwa.2011.04.009

theoretical consistency with the original Lanchester Equations, allowing for a better understanding and interpretation of the spatial modeling than the other attempts. This new space–time formulation has a potentially wider range of applications than the original LEs, such as: modeling different types of combat, politics and economic competition, bacteria control, epidemiology, predator–prey behavior, among other phenomena.

A solution is proposed using the FD method, and for situations where no regeneration of the forces is allowed a stability criterion that links the coarseness of the spatial grid and the refinement of the time-stepping is sought and found. When regeneration happens, another procedure is applied ensuring stability through a transformation that preserves the shape of the PDEs. This formulation can be regarded as another branch of the Reaction–Diffusion equations. As the purpose of this document is to give insight on a method, some simple examples are developed showing some numerical results. The examples make use of background velocity and attrition, exploring the effects of density and asymmetries. The non-negativeness of the solutions forbids analytical solutions.

The rest of this paper is organized as follows. In the next section, a general formulation of the new model and its equations are presented. The solution of the resultant linear PDE system is numerically developed using the Crank–Nicolson Method. In Section 4 the stability of the solution of the main formulation is analyzed and discussed using von Neumann characterization, that is to say, discretization is probed by assuming an amplification factor for local modes of the solutions. This method is used in conjunction with a modulation function that decouples the implicit growth effect of the concentration of forces in order to avoid misleading conclusions arising from the traditional plain application of the von Neumann analysis. An example of the model's capabilities is developed in Section 5. In Section 6 the findings are summarized, and directions for future research are discussed.

2. The model

The spatial Lanchester problem uses a spatial coordinates system for the forces that will engage in combat, typically two: the red and blue armies. Without loss of generality, the surface density of the blue forces will be represented by $B(x, y, t)$ and that of the red forces will be represented by $R(x, y, t)$. An element of each force will have an instantaneous velocity given respectively by $\vec{v}_B(x, y, t)$ and $\vec{v}_R(x, y, t)$, so the densities of current for the Blue and Red forces are $\vec{J}_B(x, y, t) = B(x, y, t)\,\vec{v}_B(x, y, t)$ and $\vec{J}_R(x, y, t) = R(x, y, t)\,\vec{v}_R(x, y, t)$. In addition, the net internal generation of forces is defined by G_B and G_R respectively. It should be highlighted that both surface densities B and R must be non-negatively valued functions, unless they have some polar behavior.

Regarding the definitions presented above, the imposition of the balance of forces (continuity) to the spatial combat leads to:

$$G_\theta - \vec{\nabla} \cdot \vec{J}_\theta = G_\theta - \frac{\partial J_{\theta x}}{\partial x} - \frac{\partial J_{\theta y}}{\partial y} = \frac{\partial \theta}{\partial t}, \tag{1}$$

where θ can be either B or R.

It remains clear that $\vec{J}_R = R \cdot \vec{v}_R$ and $\vec{J}_B = B \cdot \vec{v}_B$, where $\vec{v}_{R,B}$ is the instantaneous velocity of each part of the respective moving force, and B and R, are the densities of the Blue and Red forces respectively. Without losing generality the same equations could be extended to a volumetric combat, adding easily the z coordinate. For the purpose of this document that discussion is left out.

The internal densities can be expressed considering the profile of the engaging forces through the Lanchester expressions:

$$G_B = g_B(x, y, t) - \sum_{i=0}^{\infty} \left(\sum_{j=0}^{\infty} \alpha_{Bij} R^i B^j \right), \tag{2}$$

$$G_R = g_R(x, y, t) - \sum_{i=0}^{\infty} \left(\sum_{j=0}^{\infty} \alpha_{Rij} B^i R^j \right) \tag{3}$$

where the α coefficients might be space–time dependent.

Combining Lanchester Equations (2) and (1) and the constitutive relations for $\vec{J}_B$ a new expression arises:

$$G_B - \vec{\nabla} \cdot (B\vec{v}_B) = -\vec{\nabla} \cdot \vec{J}_B + g_B(x, y, t) - \sum_{i=0}^{\infty} \left(\sum_{j=0}^{\infty} \alpha_{Bij} R^i B^j \right) = \frac{\partial B}{\partial t} \tag{4}$$

and applying the same procedure, a twin expression results.

Thus, the general approach to model spatially Lanchester Equations can be written generically as:

$$-\vec{\nabla} \cdot (\theta \vec{v}_\theta) = \frac{\partial \theta}{\partial t} - G_\theta. \tag{5}$$

Finally, the total number of remaining forces in the battlefield for any time is described by:

$$\theta_T = \iint_S \theta(x, y, t)\, \mathrm{d}S. \tag{6}$$

Nevertheless, in order to complete the formulation, the motion behavior of the forces must be described. In some cases explicitly through the velocities, but in other cases implicitly through the densities of current, can close the problem definition. The analysis found in the next paragraphs illustrate this matter better, specifically some particular assumptions are discussed.

2.1. Responsive movement and perception

Usually in a war situation, it is expected that the motion of one of the forces, even if combats were discarded, might influence the motion of the other one. This type of movement is called responsive movement. Assuming that the density of current of forces will be related to the balance of both forces, two simple possibilities should be borne in mind as main drivers of the forces (not the only ones): linear behavior of the velocities and linear behavior of the densities of current.

The way a force reacts during the struggle may vary widely depending on the type of forces involved. Moreover, perception of the strength can be very different if it regards own forces or opposing ones. Lack of intelligence is an extreme way in the behavior of a force, but high use of the knowledge of the own and opposing motion of each side could be close to the other extreme, especially if the reaction is nonlinear.

Four parameters can be introduced here which account for a combined effect of the perception and ability of each force. The first subscript indicates the observer and the second subscript indicates the subject of the observation, e.g.: h_{BR} is the result of such a combined effect of strength of the Red force perceived by the Blue force. In order to separate both effects, it is useful to define the actual strength of each force: k_B and k_R assumed to be constants for this case, even though they could be time and terrain dependent, so four pure parameters (u_{ij}) define just perception (in general they can be time and terrain dependent), and they are defined as follows:

$$\begin{bmatrix} h_{BB} & h_{BR} \\ h_{RB} & h_{RR} \end{bmatrix} = \begin{bmatrix} k_B u_{BB} & k_R u_{BR} \\ k_B u_{RB} & k_R u_{RR} \end{bmatrix}. \tag{7}$$

As a rule of thumb, $h_{ij} = k_j u_{ij}$.

The group of forces located at some position will move towards or away from the other forces according to the perceived strength of the opponent.

$$\vec{J}_B = -\vec{f}_B - p_B \left(h_{BB} \vec{\nabla} B - h_{BR} \vec{\nabla} R \right) + B \vec{v}_{0B} \tag{8}$$

$$\vec{J}_R = -\vec{f}_R - p_R \left(h_{RR} \vec{\nabla} R - h_{RB} \vec{\nabla} B \right) + R \vec{v}_{0R} \tag{9}$$

where p_B and p_R are proportionality constants and $\vec{f}_B$ and $\vec{f}_R$ are friction terms and assumed to be constant vectors because terrain is assumed to be homogeneous. It should be pointed out that $\vec{v}_{0B}$ and $\vec{v}_{0R}$ are the background velocities of each force, that represent the strategic decision of the respective commanders. In this work, and for the sake of simplicity, these velocities are assumed to be constant vectors.

By replacing (9) into (1) and proceeding in the same way for the other forces, the densities of current no longer appear in the equations, leaving the problem with a resemblance to the classic Poisson equation in terms of the B and R force densities:

$$p_B \left(h_{BB} \nabla^2 B - h_{BR} \nabla^2 R \right) - \vec{v}_{0B} \cdot \vec{\nabla} B = \frac{\partial B}{\partial t} - G_B \tag{10}$$

$$p_R \left(h_{RR} \nabla^2 R - h_{RB} \nabla^2 B \right) - \vec{v}_{0R} \cdot \vec{\nabla} R = \frac{\partial R}{\partial t} - G_R. \tag{11}$$

Due to the right-hand side of these two equations generally this still is a nonlinear problem.

2.2. An application on the time side

The great importance of the introduction of this kind of velocity is that it exists even if no elements of the force are present at some spot. Also, because the forces would start aligning in preparation for combat or escape, quite long before.

Specifically, a responsive movement of the soldiers will be modeled. Thus, the densities of currents of the forces will move towards or away the enemies depending on the balance of gradients. In other words, each force will evaluate dynamically its strength against the opposite forces, and it will move accordingly.

Note that if friction is neglected and $h_{BB}/h_{BR} = h_{RB}/h_{RR}$, then both forces will have the same instantaneous direction at the same point of the surface, but with different signs. This condition is equivalent to having the determinant of the associated linear system equal to zero.

The situation to be analyzed assumes no spontaneous generation and only linear dependencies given by the terms:

$$\begin{aligned} \alpha_{B10} &= E_R (= k_R) \qquad \alpha_{B01} = M_B \\ \alpha_{R10} &= E_B (= k_B) \qquad \alpha_{R01} = M_R. \end{aligned} \tag{12}$$

The resulting equation can be generically written as:

$$\begin{bmatrix} \omega_1 & \omega_2 \\ \omega_3 & \omega_4 \end{bmatrix} \begin{bmatrix} B \\ R \end{bmatrix} = 0 \tag{13}$$

where

$$\omega_1 = p_B h_{BB} \nabla^2 - M_B - \left(\vec{v}_{0B} \cdot \vec{\nabla}\right) - \frac{\partial}{\partial t} \tag{14}$$

$$\omega_2 = -p_B h_{BR} \nabla^2 - E_R \tag{15}$$

$$\omega_3 = -p_R h_{RB} \nabla^2 - E_B \tag{16}$$

$$\omega_4 = p_R h_{RR} \nabla^2 - M_R - \left(\vec{v}_{0R} \cdot \vec{\nabla}\right) - \frac{\partial}{\partial t} \tag{17}$$

clearly ω_i are spatio-temporal differential operators.

3. Numerical solution for a 2D uniform grid

As B and R must be non-negatively valued for each point of the space time domain, the solution to this problem cannot be treated as in the Dirichlet or Neumann problem, because the non-negativity can be regarded as a time-dependent border condition. Bearing in mind this statement, a numerical approach suits this problem better, where the formulation given by Eq. (13) drives to a time stepping formulation for the spatial profile of the B and R scalar fields. The procedure should provide a way to adjust the time step so as to limit the maximum deviation of negative values and then to reset acceptable deviations to zero. The time stepping can be faced with a stable Crank–Nicolson (C–N) method, leaving the spatial problem to other methods. Here, Finite Differences (FD) are used as a first approach.

Eq. (13) can be rewritten as:

$$[\mathcal{L}][U] = \frac{\partial}{\partial t}[U] \tag{18}$$

where $\mathcal{L}$ is a linear matrix operator that depends on the spatial variables, and $[U] = \begin{bmatrix} B \\ R \end{bmatrix}$. Now, by rearranging terms:

$$[\mathcal{L}] = \begin{bmatrix} p_B h_{BB} \nabla^2 - M_B - \left(\vec{v}_{0B} \cdot \vec{\nabla}\right) & -p_B h_{BR} \nabla^2 - E_R \\ -p_R h_{RB} \nabla^2 - E_B & p_R h_{RR} \nabla^2 - M_R - \left(\vec{v}_{0R} \cdot \vec{\nabla}\right) \end{bmatrix} \tag{19}$$

$$[Q] = \begin{bmatrix} Q_1 & Q_2 \\ Q_3 & Q_4 \end{bmatrix} = \begin{bmatrix} p_B h_{BB} & -p_B h_{BR} \\ -p_R h_{RB} & p_R h_{RR} \end{bmatrix} \tag{20}$$

$$[W] = \begin{bmatrix} W_1 & E_2 \\ E_3 & W_4 \end{bmatrix} = \begin{bmatrix} M_B + \left(\vec{v}_{0B} \cdot \vec{\nabla}\right) & E_R \\ E_B & M_R + \left(\vec{v}_{0R} \cdot \vec{\nabla}\right) \end{bmatrix} \tag{21}$$

$$[\mathcal{L}] = [Q]\nabla^2 - [W] \tag{22}$$

$$F(U) \doteq \left\{[Q]\nabla^2 - [W]\right\}[U] = [I]\frac{\partial}{\partial t}[U] \tag{23}$$

where $E_1 = M_B$ and $E_4 = M_R$.

Crank–Nicolson decomposition leads to:

$$\frac{1}{2}\left(\left[F\left(\left[U^{n+1}\right]\right)\right] + \left[F\left(\left[U^{n}\right]\right)\right]\right) = \frac{1}{\Delta t}[I]\left(\left[U^{n+1}\right] - \left[U^{n}\right]\right), \tag{24}$$

or,

$$-[Q]\nabla^2\left[U^{n+1}\right] + \left(\frac{2}{\Delta t}[I] + [W]\right)\left[U^{n+1}\right] = [Q]\nabla^2\left[U^{n}\right] + \left(\frac{2}{\Delta t}[I] - [W]\right)\left[U^{n}\right] \tag{25}$$

and application of FD for square elements ($\Delta x = \Delta y$) for the Laplacian operator yields:

$$\nabla^2 F \sim \frac{1}{2(\Delta x)^2}\left(F_{i-1,j} + F_{i,j-1} + F_{i,j+1} + F_{i+1,j} - 4F_{i,j}\right) \tag{26}$$

that allows one to write:

$$-\frac{1}{2(\Delta x)^2}[Q]\left(\left[U_{i-1,j}^{n+1}\right]+\left[U_{i,j-1}^{n+1}\right]+\left[U_{i,j+1}^{n+1}\right]+\left[U_{i+1,j}^{n+1}\right]-4\left[U_{i,j}^{n+1}\right]\right)+\left(\frac{2}{\Delta t}[I]+[W]\right)\left[U_{i,j}^{n+1}\right]$$
$$=\frac{1}{2(\Delta x)^2}[Q]\left(\left[U_{i-1,j}^{n}\right]+\left[U_{i,j-1}^{n}\right]+\left[U_{i,j+1}^{n}\right]+\left[U_{i+1,j}^{n}\right]-4\left[U_{i,j}^{n}\right]\right)+\left(\frac{2}{\Delta t}[I]-[W]\right)\left[U_{i,j}^{n}\right]. \tag{27}$$

Now, by assuming that the grid to be considered has L by M square cells of side Δx, that $[U]$ represents a vector that holds both B and R, calling $[I_{LM}]$ the identity matrix of LM dimension, and that $[I_{2LM}]$ is the identity matrix of $2LM$ dimension, then the equation turns into:

$$\left\{\frac{2}{\Delta t}[I_{2LM}]+\begin{bmatrix}E_1[I_{LM}]+[Z_1]-\dfrac{Q_1}{2(\Delta x)^2}[S] & E_2[I_{LM}]-\dfrac{Q_2}{2(\Delta x)^2}[S]\\ E_3[I_{LM}]-\dfrac{Q_3}{2(\Delta x)^2}[S] & E_4[I_{LM}]+[Z_4]-\dfrac{Q_4}{2(\Delta x)^2}[S]\end{bmatrix}\right\}\left[U^{n+1}\right]$$
$$=\left\{\frac{2}{\Delta t}[I_{2LM}]-\begin{bmatrix}E_1[I_{LM}]+[Z_1]-\dfrac{Q_1}{2(\Delta x)^2}[S] & E_2[I_{LM}]-\dfrac{Q_2}{2(\Delta x)^2}[S]\\ E_3[I_{LM}]-\dfrac{Q_3}{2(\Delta x)^2}[S] & E_4[I_{LM}]+[Z_4]-\dfrac{Q_4}{2(\Delta x)^2}[S]\end{bmatrix}\right\}\left[U^{n}\right] \tag{28}$$

where $[S]$ is the matrix generated from the assembly given by the Laplacian operator,

$$[Z_1]=v_{0Bx}[X]+v_{0By}[Y] \tag{29}$$

and

$$[Z_4]=v_{0Rx}[X]+v_{0Ry}[Y] \tag{30}$$

where $[X]$ and $[Y]$ are generated by using respectively the differential operators given by:

$$\frac{\partial H}{\partial x}\sim\frac{1}{2(\Delta x)}\left(H_{i+1,j}-H_{i-1,j}\right) \tag{31}$$

$$\frac{\partial H}{\partial y}\sim\frac{1}{2(\Delta x)}\left(H_{i,j+1}-H_{i,j-1}\right). \tag{32}$$

Clearly, Eq. (28) gives an iterative procedure to solve $[U]$ by stepping. Eq. (28) presents separately the time and spatial evolution of the forces. Indeed, if $[Q_i=0]$, then the system becomes the traditional Lanchester model, without a spatial component.

As expected, all the terms in the matrices are constant and hopefully positive. If a negative but tolerable value, i.e. small enough, appears in one of the components of the vector $\binom{B}{R}$ then that negative term must be replaced by a zero because only positive forces are significant here. If for some element of that vector the negative value is too large, then it is advisable to repeat the procedure for the last step with a smaller value of Δt.

4. Stability

4.1. No regeneration

Time stepping of the equations for the linear case leads to:

$$\left[\left(\frac{2}{\Delta t}I+E\right)-Q\nabla^2\right]U^{n+1}=\left[\left(\frac{2}{\Delta t}I-E\right)-Q\nabla^2\right]U^{n}. \tag{33}$$

On the other side, the Laplacian operator under Crank–Nicolson becomes:

$$\nabla^2U\sim\frac{1}{2(\Delta x)^2}\left\{U_{i-1,j}+U_{i,j-1}+U_{i,j+1}+U_{i+1,j}-4U_{i,j}\right\}. \tag{34}$$

So the equations under analysis become:

$$\left(\frac{2}{\Delta t}+E_1-Q_1\nabla^2\right)B^{n+1}+\left(E_2-Q_2\nabla^2\right)R^{n+1}=\left(\frac{2}{\Delta t}-E_1+Q_1\nabla^2\right)B^{n}+\left(-E_2+Q_2\nabla^2\right)R^{n} \tag{35}$$

and

$$\left(\frac{2}{\Delta t}+E_4-Q_4\nabla^2\right)R^{n+1}+\left(E_3-Q_3\nabla^2\right)B^{n+1}=\left(\frac{2}{\Delta t}-E_4+Q_4\nabla^2\right)R^{n}+\left(-E_3+Q_3\nabla^2\right)B^{n}. \tag{36}$$

Now assuming a local mode solution, which employs *von Neumann stability analysis* with the *Lax method*, as in [26], and extended to a two-functions system, the problem remains stable if the amplitude of the local modes is kept bounded because the assumption of local modes $U_{j,l}^{n} = \begin{bmatrix}\xi \\ \eta\end{bmatrix} \rho^{n} \mathrm{e}^{\mathrm{i}(jk_x+lk_y)\Delta x}$ imply that the relative amplitude ρ, should comply with $\rho < 1$, because the time dependence of the relative amplitude of the local modes is represented by the successive integer powers of ρ. Bearing that in mind, it is possible to write:

$$\left(\begin{bmatrix}\frac{2}{\Delta t}+E_1 & E_2 \\ E_3 & \frac{2}{\Delta t}+E_4\end{bmatrix} - \begin{bmatrix}Q_1 & Q_2 \\ Q_3 & Q_4\end{bmatrix}\nabla^2\right)\begin{bmatrix}\rho^{n+1}\xi \\ \rho^{n+1}\eta\end{bmatrix}\mathrm{e}^{\mathrm{i}(jk_x+lk_y)\Delta x}$$
$$= \left(\begin{bmatrix}\frac{2}{\Delta t}-E_1 & -E_2 \\ -E_3 & \frac{2}{\Delta t}-E_4\end{bmatrix} + \begin{bmatrix}Q_1 & Q_2 \\ Q_3 & Q_4\end{bmatrix}\nabla^2\right)\begin{bmatrix}\rho^{n}\xi \\ \rho^{n}\eta\end{bmatrix}\mathrm{e}^{\mathrm{i}(jk_x+lk_y)\Delta x}. \tag{37}$$

But the Laplacian, applied to the exponential, with $\Delta x = \Delta y$ gives the following result:

$$\nabla^2 \sim \frac{1}{2\,(\Delta x)^2}\left\{\mathrm{e}^{\mathrm{i}k_x\Delta x} + \mathrm{e}^{-\mathrm{i}k_x\Delta x} + \mathrm{e}^{\mathrm{i}k_y\Delta x} + \mathrm{e}^{-\mathrm{i}k_y\Delta x} - 4\right\}\mathrm{e}^{\mathrm{i}(jk_x+lk_y)\Delta x} \tag{38}$$

$$\nabla^2 \sim \frac{1}{(\Delta x)^2}\left\{\cos k_x\Delta x + \cos k_y\Delta x - 2\right\}\mathrm{e}^{\mathrm{i}(jk_x+lk_y)\Delta x} = \frac{\alpha}{(\Delta x)^2}\mathrm{e}^{\mathrm{i}(jk_x+lk_y)\Delta x} \tag{39}$$

also:

$$\vec{v}_0\cdot\vec{\nabla} \sim \frac{\mathrm{i}}{\Delta x}\left(v_{0x}\sin k_x\Delta x + v_{0y}\sin k_y\Delta x\right) \tag{40}$$

$$\left(\begin{bmatrix}\frac{2}{\Delta t}+W_1 & E_2 \\ E_3 & \frac{2}{\Delta t}+W_4\end{bmatrix} - \frac{\alpha}{(\Delta x)^2}\begin{bmatrix}Q_1 & Q_2 \\ Q_3 & Q_4\end{bmatrix}\right)\begin{bmatrix}\rho^{n+1}\xi \\ \rho^{n+1}\eta\end{bmatrix}$$
$$= \left(\begin{bmatrix}\frac{2}{\Delta t}-W_1 & -E_2 \\ -E_3 & \frac{2}{\Delta t}-W_4\end{bmatrix} + \frac{\alpha}{(\Delta x)^2}\begin{bmatrix}Q_1 & Q_2 \\ Q_3 & Q_4\end{bmatrix}\right)\begin{bmatrix}\rho^{n}\xi \\ \rho^{n}\eta\end{bmatrix} \tag{41}$$

but the vector on the left-hand side of the equation can be written as a simple operation over the same vector found on the other side of the equation:

$$\left\{\left(\begin{bmatrix}\frac{2}{\Delta t}+W_1 & E_2 \\ E_3 & \frac{2}{\Delta t}+W_4\end{bmatrix} - \frac{\alpha}{(\Delta x)^2}\begin{bmatrix}Q_1 & Q_2 \\ Q_3 & Q_4\end{bmatrix}\right)\begin{bmatrix}\rho & 0 \\ 0 & \rho\end{bmatrix}\right\}\begin{bmatrix}\rho^{n}\xi \\ \rho^{n}\eta\end{bmatrix}$$
$$-\left\{\begin{bmatrix}\frac{2}{\Delta t}-W_1 & -E_2 \\ -E_3 & \frac{2}{\Delta t}-W_4\end{bmatrix} + \frac{\alpha}{(\Delta x)^2}\begin{bmatrix}Q_1 & Q_2 \\ Q_3 & Q_4\end{bmatrix}\right\}\begin{bmatrix}\rho^{n}\xi \\ \rho^{n}\eta\end{bmatrix} = 0. \tag{42}$$

And as the valid results need a nontrivial solution, the determinant of the involved matrix must be nil. Rewriting the matrix, the expression is now:

$$\det\begin{bmatrix}\left(\frac{2}{\Delta t}\right)(\rho-1) + \left(E_1 - \frac{\alpha Q_1}{(\Delta x)^2}\right)(\rho+1) & \left(E_2 - \frac{\alpha Q_2}{(\Delta x)^2}\right)(\rho+1) \\ \left(E_3 - \frac{\alpha Q_3}{(\Delta x)^2}\right)(\rho+1) & \left(\frac{2}{\Delta t}\right)(\rho-1) + \left(E_4 - \frac{\alpha Q_4}{(\Delta x)^2}\right)(\rho+1)\end{bmatrix} = 0. \tag{43}$$

Which leads to:

$$\left\{\left(\frac{2}{\Delta t}\right)(\rho-1) + \left(W_1 - \frac{\alpha Q_1}{(\Delta x)^2}\right)(\rho+1)\right\}\left\{\left(\frac{2}{\Delta t}\right)(\rho-1) + \left(W_4 - \frac{\alpha Q_4}{(\Delta x)^2}\right)(\rho+1)\right\}$$
$$= \left\{\left(E_2 - \frac{\alpha Q_2}{(\Delta x)^2}\right)(\rho+1)\right\}\left\{\left(E_3 - \frac{\alpha Q_3}{(\Delta x)^2}\right)(\rho+1)\right\}. \tag{44}$$

This is a second order equation that must guarantee that both solutions of $|\rho|$ are smaller than one. It should be noticed from Eq. (39) that always:

$$-4 \leq \alpha \leq 0, a \tag{45}$$

result that can be helpful when the background velocities are zeroes.

Returning to the second degree equation for ρ. If the following parameters are defined, then it can be compactly written:

$$a_l = W_l - \frac{\alpha Q_l}{(\Delta x)^2} \tag{46}$$

for $l = 1, 2, 3, 4$ where:

$$W_1 = E_1 + \mathrm{i}\beta_B \tag{47}$$

$$W_2 = E_2 \tag{48}$$

$$W_3 = E_3 \tag{49}$$

$$W_4 = E_4 + \mathrm{i}\beta_R \tag{50}$$

and,

$$\beta_B = \left(\frac{1}{\Delta x}\right)\left(v_{0Bx} \sin k_x \Delta x + v_{0By} \sin k_y \Delta x\right) \tag{51}$$

$$\beta_R = \left(\frac{1}{\Delta x}\right)\left(v_{0Rx} \sin k_x \Delta x + v_{0Ry} \sin k_y \Delta x\right) \tag{52}$$

$$b = \frac{2}{\Delta t} \tag{53}$$

$$c = \frac{\alpha}{(\Delta x)^2} \tag{54}$$

$$A = \left\{\frac{(a_1a_4 - a_2a_3 - \beta_B\beta_R) - b^2 + \mathrm{i}\,(a_1\beta_R + a_4\beta_B)}{b^2 + (a_1a_4 - a_2a_3 - \beta_B\beta_R) + b\,(a_1 + a_4) + \mathrm{i}\,(a_1\beta_R + a_4\beta_B + b\,(\beta_B + \beta_R))}\right\} \tag{55}$$

$$D = \left\{\frac{b^2 + (a_1a_4 - a_2a_3 - \beta_B\beta_R) - b\,(a_1 + a_4) + \mathrm{i}\,(a_1\beta_R + a_4\beta_B - b\,(\beta_B + \beta_R))}{b^2 + (a_1a_4 - a_2a_3 - \beta_B\beta_R) + b\,(a_1 + a_4) + \mathrm{i}\,(a_1\beta_R + a_4\beta_B + b\,(\beta_B + \beta_R))}\right\}. \tag{56}$$

Both A and D can be complex numbers, giving:

$$\rho^2 + 2A\rho + D = 0. \tag{57}$$

Thus, two conditions should be met for stability:

$$\|\rho_1\| = \left\|-A + \sqrt{A^2 - D}\right\| < 1 \tag{58}$$

and:

$$\|\rho_2\| = \left\|A + \sqrt{A^2 - D}\right\| < 1. \tag{59}$$

If $\vec{v}_{0B}$ and $\vec{v}_{0R}$ are not zero, then it is useful to define two variables $\varphi = k_x\Delta x$ and $\psi = k_y\Delta x$ where both range from 0 to 2π, and then plot the expressions for $1 - \|\rho_1\|$ and $1 - \|\rho_2\|$. Both surfaces should be constrained between 0 and 1 for assured stability.

It is usually possible to find suitable parameters for the simulation that can guarantee full satisfaction of both conditions, and hence stability.

If the velocities $\vec{v}_{0B}$ and $\vec{v}_{0R}$ are both zero, the stability is more easily guaranteed using the α parameter as the variable for plotting, now as a line sketch, the behavior of $1 - \|\rho_1\|$ and $1 - \|\rho_2\|$.

4.2. Self regeneration of one or more forces

Assuming that one of the forces has the biggest negative value for M_p, where p can be either B or R, and just for this example, $p = R$ and $K = -M_R$, by taking Eq. (13) and replacing the concentrations for the following functions:

$$B = b\exp(st) \tag{60}$$

and

$$R = r\exp(st) \tag{61}$$

Table 1
Initial conditions.

θ	R	B	R	B	R	B
Amplitude	6000	10,000	6000	10,000	6000	10,000
A_θ	4.2	4	4.2	4	4.2	4
$c_{x\theta}$	453.00	153.85	453.00	153.85	453.00	153.85
$c_{y\theta}$	142.37	180.37	142.37	180.37	142.37	180.37
$x_{0\theta}$	1909.80	2068.95	1697.60	2068.95	1485.40	2068.95
$y_{0\theta}$	1007.95	2122.00	1007.95	2122.00	1007.95	2122.00

the time derivative allows one to write:

$$\begin{bmatrix} p_B h_{BB}\nabla^2 - (s + M_B) - \left(\vec{v}_{0B}\cdot\vec{\nabla}\right) & -p_B h_{BR}\nabla^2 - E_R \\ -p_R h_{RB}\nabla^2 - E_B & p_R h_{RR}\nabla^2 - (s - K) - \left(\vec{v}_{0R}\cdot\vec{\nabla}\right) \end{bmatrix} \begin{bmatrix} b \\ r \end{bmatrix} - \frac{\partial}{\partial t}\begin{bmatrix} b \\ r \end{bmatrix} = 0 \tag{62}$$

which means that if the value chosen for s is greater than K, the equation keeps the same shape as (13) but replacing the old value of M_B by the new value of $s + M_B$. It follows now, that the value of $-K$ in the system for B and R which renders the equations unstable, is replaced for $s - K$ in the system for b and r, leading to a stable solution.

This formulation sorts out the problem guaranteeing stability for $\binom{b}{r}$, using the same numerical formulation, so the real solution is obtained by simply multiplying that vector by $\exp(st)$, since the solution has been obtained after having chosen $s > K$. Also, this method can help in reducing the size of the grid in $x - y$ or the stepping in t, even for non-regenerating relations between the functions. It is very important to highlight that the spatial envelope of the solutions for B and R do not change, so for a given time of evolution, the distribution of forces b and r is the same as for B and R, except for the exponential factor.

5. Numerical illustration

5.1. Modeling troop movement tactics

"*Invincibility lies in the defense; the possibility of victory in the attack. One defends when his strength is inadequate; he attacks when it is abundant*."—Sun Tzu.

Let us assume two disciplined (i.e.: low level of dispersion among the army contingent) and well-informed (i.e.: both have perfect foresight of their own and of the enemy forces) armies that fight for the control of a well-defined area. The red army is in a stationary position, protecting the area of interest, while the blue army is moving towards it. The blue army is less numerous than the red one, but it could choose the time and location of its attack. Logically, the best tactic to follow for the blue army would be to take advantage of the attack location, choosing a zone of asymmetry, where they can locally overpower the red army forces. Thus, *the main objective of the blue army is to cause the greater damage to the enemy forces at a minimum cost of its own casualties*. Our general formulation, a spatial Lanchester model, will allow us to model this battle in a proper way, ensuring consistency and stability in the results.

The model uses a square grid of 77 nodes on each side. The initial distribution functions share the same symmetry, but different initial spatial amplitude and location. Abrupt changes in the initial state of the system are avoided by using the following functions as initial conditions:

$$\theta\,(x, y, t = 0) = A_\theta \cdot \operatorname{sech}\left(\left(\frac{x - x_{0\theta}}{c_{x\theta}}\right)^2 + \left(\frac{y - y_{0\theta}}{c_{y\theta}}\right)^2\right) \tag{63}$$

where A_θ is the amplitude of the length of θ forces, xy are locations points, and c is the length of one side of each cell. The parameters of the expressions given by (63) are presented in Table 1.

The main arbitrary and physical units used in the simulation are presented in Table 2:

The experiment considers different locations for the blue army attack, starting nearly from the center of the grid and moving towards the left far side of the red forces. The reference system has their coordinates (0, 0) located at the bottom-left corner of the grid. Coordinates are measured in meters. In particular, four runs are presented: (1) $R36$ where the blue army begins its attack in coordinate $x = 1909.8$ m, or equivalently in line 36 according to our grid definition, (2) $R32$ that starts the attack at coordinate $x = 1697.6$, in line 32, (3) $R28$ where the attack starts at coordinate $x = 1485.4$, line 28; and finally, (4) $RD28$ that commences in the same coordinate $x = 1485.4$ as in the previous one, but with a different discipline of attack, in this case with more diffusion, see the quotient lower bound in Table 1. The scenario $RD28$ is set with 0.75 instead of 0.35 as all the other three previous simulations. In Fig. 1, the battle is simulated for each scenario in turn, showing the evolution of red and blue forces.

The results are shown in the table below, where R_{fi} and B_{fi} are the ratios of the final and initial forces at the same time once the battle has started, specifically at 1400 time steps, or in other words at 63 min according to the units already presented in Table 2.

Table 2
Equivalences and units.

Concept	Arbitrary unit	Physical unit
Time	UT	180 (min)
Distance	UL	$7.2 \cdot 10^4$ (m)
Cell side	$7.368 \cdot 10^{-4}$ UL	53.05 (m)
Time step	$0.25 \cdot 10^{-3}$UT	$45 \cdot 10^{-3}$ (min)
Soldiers	US	10^4 (soldier)
Concentration of forces (B; R)	$\mathrm{UC} = \mathrm{US} \cdot \mathrm{UL}^{-2}$	$1.929 \cdot 10^{-6}$ (soldier m^{-2})
Velocity ($\vec{v}$) or Speed (v)	$\mathrm{UV} = \mathrm{UL} \cdot \mathrm{UT}^{-1}$	400 (m min^{-1})
Density of current ($\vec{J}$)	$\mathrm{UJ} = \mathrm{US} \cdot \mathrm{UL}^{-1}\ \mathrm{UT}^{-1}$	$7.716 \cdot 10^{-5}$ (soldier m^{-1} min^{-1})
p_B	10^{-7} UL^2	518.4 (m^2)
$p_{R\mathrm{case1}}$	10^{-7} UL^2	518.4 (m^2)
$p_{R\mathrm{case2}}$	$5 \cdot 10^{-7}$ UL^2	2592 (m^2)
M_B	0.0 UT^{-1}	0 (min^{-1})
E_R	5.5 UT^{-1}	0.03056 (min^{-1})
M_R	0.0 UT^{-1}	0 (min^{-1})
E_B	5.5 UT^{-1}	0.03056 (min^{-1})
v_{0B}	$\frac{3}{40}$ UV	30 (m min^{-1})
Run length	1400 Time steps	63 (min)

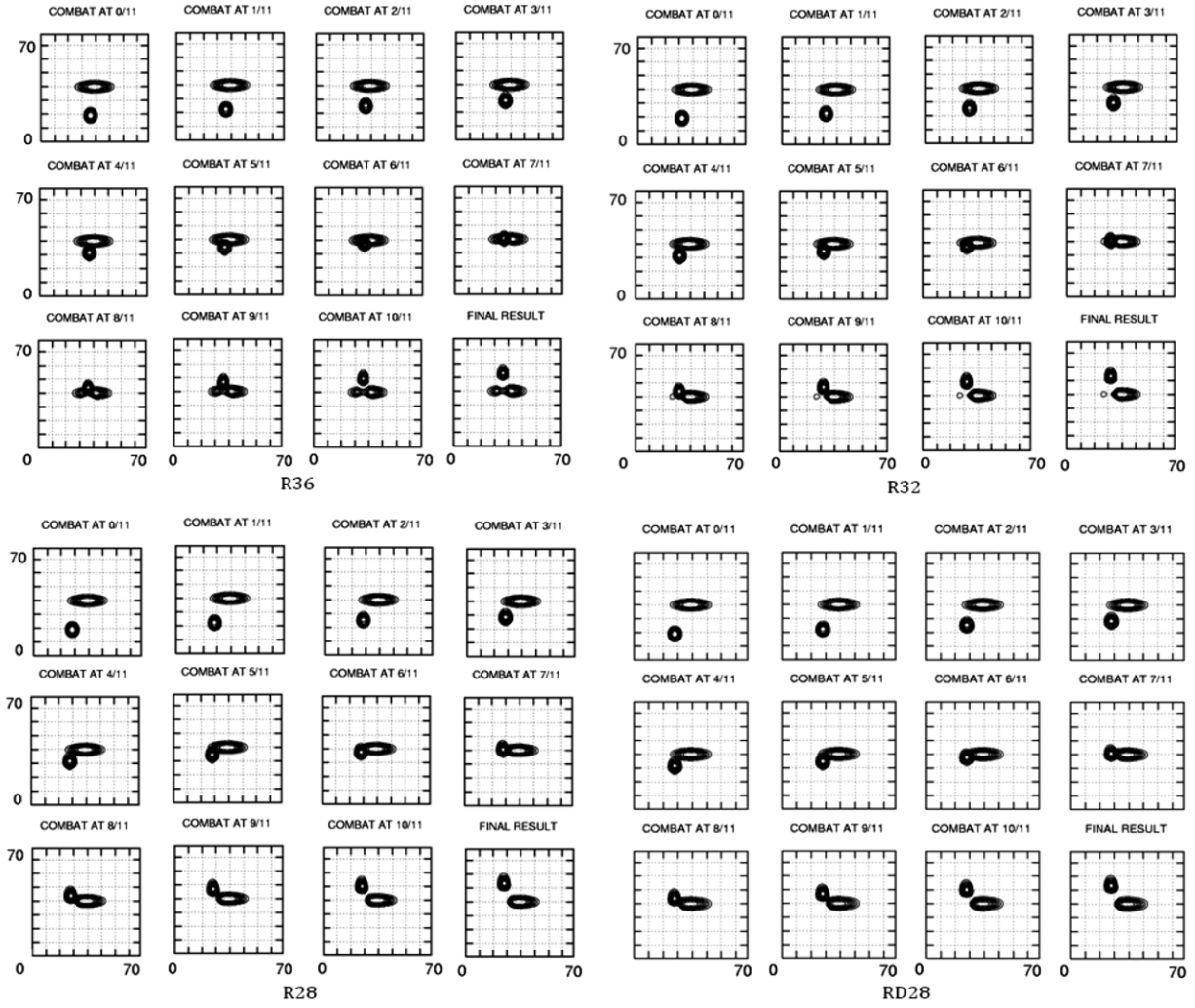

Fig. 1. Evolution of red and blue forces at different times and starting positions—contour plots. (For interpretation of the references to colour in this figure legend, the reader is referred to the web version of this article.)

Table 3
Simulations scenarios and results: Percentage of losses. $R_i/B_i = 1.3670$.

Case	Label	Simulation scenarios	R_{fi}	B_{fi}	R_{fi}/B_{fi}	R_f/B_f
1	*R*36	Attack at $x = 1910$ (m)	0.726009	0.729386	0.995370	1.3607
1	*R*32	Attack at $x = 1698$ (m)	0.759713	0.841087	0.903251	1.2348
1	*R*28	Attack at $x = 1485$ (m)	0.874933	0.970228	0.901780	1.2327
2	*RD*28	Reduced discipline	0.859049	0.973607	0.882336	1.2062

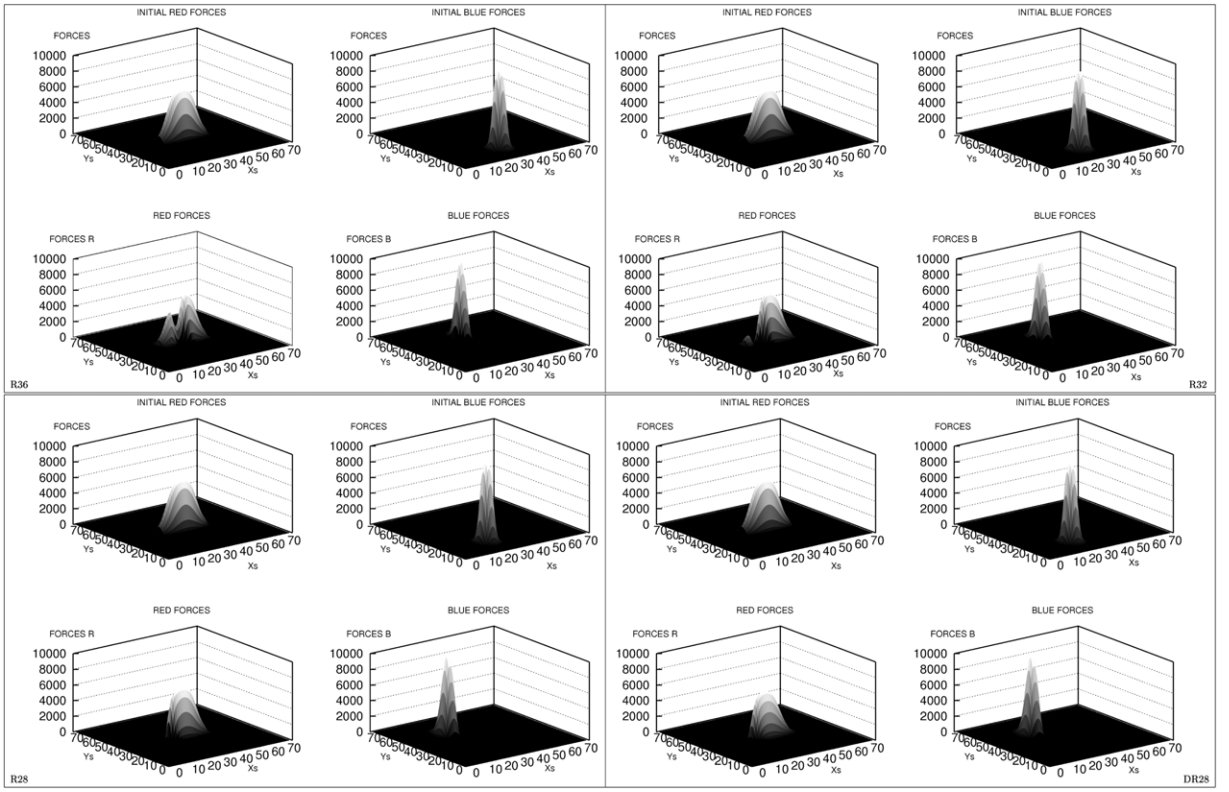

Fig. 2. Evolution of red and blue forces at different times and starting positions—3D plots. (For interpretation of the references to colour in this figure legend, the reader is referred to the web version of this article.)

Considering the objective of the blue forces, *to cause the greater damage to the enemy forces at a minimum cost of its own casualties*, and Table 3, the best strategy would be that with the lower R_f/B_f coefficient, which is a measure of the balance of forces.

Clearly the scenario where more red forces are destroyed is *R*36, with almost 30% of losses regarding its initial number, however, about the same proportion of the blue army is also eliminated. This situation is undesirable if more attacks are intended in order to conquer the land where the red army stays, unless reinforcements are available for the attackers when splitting the army into two parts, see Fig. 2.

If the attack is shifted away from the symmetry line of the defending forces while keeping the same formation, the situation improves in terms of force balances. The results suggests that the best place for the blue attack, where full advantage is taken from the asymmetry, is the scenario *R*28, where almost 13% of the red army's initial forces are destroyed, but only 3% of the blue forces are eliminated. Actually, the R_f/B_f coefficient gets better and hints at the convenience of another attack following the same tactics on the other flank of the red army.

Another analysis is done assuming that the discipline of the blue army formation is relaxed, or in other words the constant of diffusion is greater than before for the blue army, scenario *RD*28. The results point towards the convenience of this tactic, certainly a more realistic one, showing that the troops discipline (cohesion), when this type of attack is performed, must be carefully designed because what underlies here is a chasing behavior that can render good results only when the local balance of forces keeps the asymmetry of the battle. If the formation discipline gets even more lax, then a disastrous defeat could be faced by the blue army.

In the case analyzed here, and assuming no other interactions, after 63 min almost 15% of the red forces are eliminated but less than 3% of the blue forces are down, thus improving the result with respect to a more stern formation discipline.

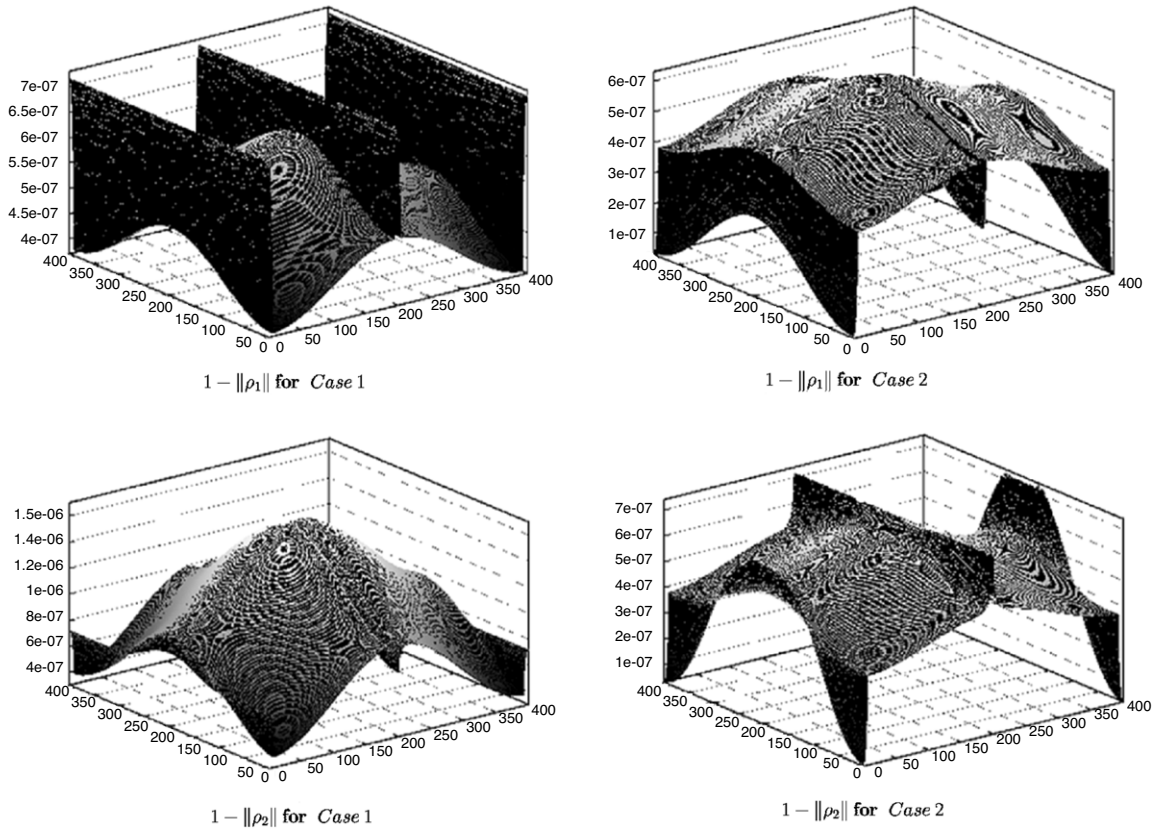

Fig. 3. Stability coefficients $1 - \|\rho_1\|$ and $1 - \|\rho_2\|$ for the simulations *R*28, *R*32 and *R*36 (case 1) and *RD*28 (case 2). Exponential constant $S = 0.6$.

Clearly, these results seem to confirm the fact that a good tactic in this situation could be to take advantage of the asymmetry repeatedly, slicing the enemy army, until a full attack at the center is feasible in order to achieve the annihilation of the opposite army. A future research could be to optimize the path and number of attacks, in a way the time and the human losses are reduced. Another area of future research is to analyze different angles of attacks and speeds, which are allowed by the present general formulation. However, in this case, given the great amount of computational resources needed to perform the necessary interpolations, this aspect of the modeling has not been considered.

5.2. Stability analysis

Stability, which is explained in 4, is assured for the parameters given in all the previous example. The bi-valued coefficient $1 - |\rho|$ is shown for 160,000 points, hence exploring the full range of angles ($0 \longleftrightarrow 2\pi$) with a reasonable refinement. The analysis results in a rather stable solution, as can be seen in Fig. 3, where the $1 - |\rho|$ coefficient is always greater than zero and far below one. The result is guaranteed only because an attenuation/amplification process using $S = 6.0$ has been used for the *B* and *R* functions, otherwise the solutions had been unreliable due to divergence during time-stepping.

It is important to notice that for smaller grids some inconsistencies in the integration process were found. Specifically, for example, when a square grid of 57×57 nodes was used, the continuity of the attacking forces experienced up to 3% of fluctuations, due to velocity-interpolation effects. When the grid is expanded to 77×77 nodes, the fluctuation is reduced to 1%, a figure that reflects a better matching of the grid with the concentration of the blue forces while they move, mainly due to the background velocity.

6. Concluding remarks

A new formulation for solving the spatial modeling of Lanchester Equations is presented. Particularly, this new model is conceptualized on the basis of a consistent balance of forces and developed in order to account not only for the time dynamics of the problem, but also for the location, movement and concentrations of the forces at "war". In contrast with other attempts, the model solved here, ensures stability and theoretical consistency with the original Lanchester Equations, allowing for a better understanding and interpretation of the spatial modeling. The model involves a system of PDEs similar

to those of Reaction–Diffusion equations, and its solutions can be found using Finite Differences, Finite Elements or other numerical methods.

In order to find stable solutions, the method provides stability indices that can hint to the programmer new space–time discretizations, but also the procedure can introduce an exponential factor that can ensure stability for naturally growing forces under this numerical method.

As the non-negativeness of the solutions forbids analytical solutions, insight is given through a simple example that is developed showing some numerical results. Stability has been checked for one of the force's behavior and a non divergent solution is rather guaranteed for both regenerating and non-regenerating forces.

The results of the LEs are expanded by these new modeling possibilities in a number of directions, giving to the analysis a whole new spectrum of variables and parameters to simulate in a more realistic fashion the current problems modeled with LEs.

As a numerical illustration of the general spatial Lanchester model presented in this research, a simple combat situation is simulated. Specifically, a troop looks for the best location (more efficient) to attack a stationary army which protects a site. The model is aimed to simulate different troop movement tactics that allow the invaders to provoke maximum damage at a minimum cost. The main results confirm the fact that spatial modeling matters and that in this specific setting a good tactic could be to attack the less dense zone in order to take advantage of the asymmetry achieved in that specific location.

As future research, optimal path could be found by varying angles of attack, either keeping or modifying the formation and repeating the assault, giving important information in terms of the more effective tactics.

The general formulation introduced here could also have stochastic analysis, either by specifically modeling the background velocity field or by means of a characterization of the term that accounts for the struggle. In addition, the model could be applied to 3D situations, requiring of course more computational resources but little analytical effort.

Despite the fact that this general model is used here for warfare applications, there is a variety of spatial problems where this model could be used, e.g.: epidemiology and public health policy, spatial retail competition, crime location and public control policy and others where there are two or more struggling forces.

References

[1] F. Lanchester, Aircraft in Warfare: The Dawn of the Fourth Arm, Constable, London, 1916.
[2] P.M. Morse, G.E. Kimball, Methods of Operations Research, first ed. revised ed., Peninsula Publishing, 1970, P.O. Box 867, Los Altos, California, 1950, tenth Printing.
[3] J. Engel, A verification of Lanchester law, Journal of the Operations Research Society of America 2 (2) (1953) 163–171.
[4] R.J.E. Bach, L. Dolanský, H.L. Stubbs, Some recent contributions to the Lanchester theory of combat, Operations Research 10 (3) (1962) 314–326.
[5] P.S. Chen, P. Chu, Applying Lanchester's linear law to model the Ardennes campaign, Naval Research Logistics 48 (8) (1991) 653–661.
[6] G. Kaup, D. Kaup, N. Finkelstein, The Lanchester (n, 1) problem, Journal of the Operational Research Society 56 (2005) 1399–1407.
[7] C.-Y. Hung, G. Yang, P. Deng, T. Tang, S.-P. Lang, P. Chu, Fitting Lanchester's square law to the Ardennes campaign, Journal of the Operational Research Society 56 (8) (2005) 942–946.
[8] J.G. Taylor, Lanchester Models of Warfare, in: Research Monographs, Operations Research Society of America, 1983.
[9] E. Adams, M. Mesterson-Gibbons, Lanchester's attrition models and fights among social animals, Behavioral Ecology 14 (5) (2003) 712–723.
[10] J. Gani, Some problems of epidemic theory, Journal of the Royal Statistical Society: Series A 141 (3) (1978) 323–347.
[11] A. Lacasta, I. Cantalapiedra, C. Auguet, A. Peñaranda, L. Ramírez-Piscina, Modelling of spatio-temporal patterns in bacterial colonies, Physical Review E 59 (59) (2008) 7036–7041.
[12] N. Mabrouk, G. Deffuant, C. Lobry, M2m third international model-to-model workshop, in: Confronting macro, meso and micro scale modelling of bacteria dynamics, 2007.
[13] G.E. Kimball, Some industrial applications of military operations research methods, Operations Research 5 (2) (1957) 201–204.
[14] G. Erickson, Dynamic Models of Advertising Competition, Kluwer Academic Publishers, 1991.
[15] G.M. Erickson, Note. Dynamic conjectural variations in a Lanchester oligopoly, Management Science 43 (11) (1997) 1603–1608.
[16] J. Jarrar, G. Martín-Herrán, G. Zaccour, Markov perfect equilibrium advertising strategies of Lanchester duopoly model: a technical note, Management Science 50 (7) (2004) 995–1000.
[17] P.K. Chintagunta, N.J. Vilcassim, An emprical investigation of advertising strategies in a dynamic duopoly, Management Sciences 38 (9) (1992) 1230–1244.
[18] J. Hirshleifer, Economics from a biological viewpoint, Journal of Law and Economics 20 (1) (1977) 1–52.
[19] J. Hirshleifer, The technology of conflict as an economic activity, American Economic Review 81 (2) (1991) 130–134. papers and Proceedings of the Hundred and Third Annual Meeting of the American Economic Association.
[20] J. Hirshleifer, The macrotechnology of conflict, Journal of Conflict Resolution 44 (6) (2000) 773–792.
[21] H.M. Neary, Equilibrium structure in an economic model of conflict, Economic Inquiry 35 (3) (1997) 480–494. published Online: 2007.
[22] V. Protopopescu, R. Santoro, J. Dockery, Combat modeling with partial differential equations, European Journal of Operational Research 38 (1989) 178–183.
[23] C. Cosner, S. Lenhart, V. Protopopescu, Parabolic systems with nonlinear competitive interactions, IMA Journal of Applied Mathematics 44 (1990) 285–298.
[24] R.S. Cantrell, C. Cosner, Models for predator–prey systems at multiple scales, SIAM Review 38 (2) (1996) 256–286.
[25] E. Crooks, E. Dancer, D. Hilhorst, M. Mimura, H. Ninomiya, Spatial segregation limit of a competition–diffusion system with dirichlet boundary conditions, Nonlinear Analysis. Real World Applications 5 (2004) 645–665.
[26] W.H. Press, B.P. Flannery, S.A. Teukolski, W.T. Vetterling, Numerical Recipes: The Art of Scientific Computing, Press Syndicate of the University of Cambridge, 1989.